Brain Stroke Monitoring via a Low-complexity Microwave Scanner: Realistic Multi-tissue Head Phantom Validation

David O. Rodriguez-Duarte
Dept. of Electronics and Telecommunications
Politecnico di Torino
Torino, Italy
david.rodriguez@polito.it

Jorge A. Tobon Vasquez
Dept. of Electronics and Telecommunications
Politecnico di Torino
Torino, Italy
jorge.tobon@polito.it

Martina Gugliermino
Dept. of Electronics and Telecommunications
Politecnico di Torino
Torino, Italy
martina.gugliermino@polito.it

Cristina Origlia
Dept. of Electronics and Telecommunications
Politecnico di Torino
Torino, Italy
cristina.origlia@polito.it

Valeria Mariano
Dept. of Electronics and Telecommunications
Politecnico di Torino
Torino, Italy
valeria_mariano@polito.it

Rosa Scapaticci
Institute for Electromagnetic Sensing of the Environment
National Research Council
Naples, Italy
scapaticci.r@irea.cnr.it

Lorenzo Crocco
Institute for Electromagnetic Sensing of the Environment
National Research Council
Naples, Italy
crocco.l@irea.cnr.it

Francesca Vipiana
Dept. of Electronics and Telecommunications
Politecnico di Torino
Torino, Italy
francesca.vipiana@polito.it

***Abstract*—The growing figures of brain stroke impact on the global population, especially in low-to-middle-income countries, and its severe short and long-term medical repercussions have raised the demand for additional technological solutions that support the specific medical needs and efforts against those. This work presents a tailored low-complexity microwave-based scanner designed for monitoring the after-onset stroke, and its experimental validation on anthropomorphic multi-tissue head phantoms, mimicking realistic clinical conditions. The system exploits microwaves' non-invasive and harmless nature and the existing high-performance microwave hardware and computing power to generate dynamically tridimensional qualitative maps signaling and tracking the stroke-affected areas. The hardware component consists of multi-view architecture using a 22-antenna helmet illuminating the studied domain with low-power electromagnetic waves working at around 1 GHz. To enable real-time operation with a low computing demand image formation is performed via a linear inversion algorithm based on the distorted Born approximation.**

***Index Terms*—Biomedical microwave imaging, brain stroke monitoring, inverse scattering, phantoms.**

I. Introduction

Brain stroke a leading cause of death and lifelong disability, which affects more than twelve million people yearly worldwide, of whom around 90% reside in low-to-middle-income countries [1], [2], and with a tendency to worsen considering the forecast aging of the population. It is a critical medical emergency provoked by blood-flow alterations, which induce a lack of oxygenation and nourishment that kills millions of neurons per second. Hence, a prompt medical intervention is pivotal to increasing the survival rate and the recovery chances. Technically, an acute event arises from blood flow impairment due to either a brain artery rupture or leakage or a blood clot limiting tissue perfusion, hemorrhagic (HS), and ischemic (IS) strokes, respectively. In both cases, stroke implies dead tissue, but they require different specific treatments, and a wrong diagnosis could be deadly for patients. In this context, the medical needs can be enclosed into two families: first, the early diagnosis. i.e., detection and classifications, prompt medical stabilization, and, second, a tailored treatment and follow-up condition that can then be transferred and addressed through the medical stroke-intervention protocols.

Accordingly, physicians support intervention stages on different technological solutions, where gold standard imaging-based ones such as Magnetic Resonance Imaging (MRI) or X-ray-based Computerized Tomography (CT) play a crucial role during the diagnosis and monitoring. These solutions indicate the location and shape of the stroke, as well as its nature, partially fulfilling the medical needs. Considering the limitations of current technologies, in the last years, microwave imaging (MWI) has emerged as an attractive nonionizing, low-intensity, and cost-effective complementary alternative solution able to fill the gaps in prehospital diagnosis of the stroke, bedside brain imaging, and continuous monitoring during the post-acute stage, albeit at the cost of a lower resolution.

MWI systems take advantage of the dielectric contrast between healthy and affected tissues when illuminated with electromagnetic (EM) waves at microwave frequencies. In an HS, the electrical properties of the stroke-affected tissue increase due to the bleeding. Conversely, the EM properties decrease during an IS due to the reduction of oxygen-rich blood flow. In general, this technology is a good candidate for problems that require favorable penetration depth, like the head case, while offering a convenient framework for continuous monitoring scenarios considering the harmfulness of microwaves. Moreover, MWI devices exploit the current high-performance microwave hardware and computing power to solve the inverse scattering problem behind the imaging job. In addition to technical advantages, it also provides mobile and low-cost imaging platforms, supported on the last

the mobile industry and microwave device advancements.

A MWI device typically employs an array of transmitting-receiving antennas gathering the back-scattered wave data proving the body under test, which is later employed by a data processing algorithm to map the dielectric contrast within the body. It is found in applications such as imaging breast cancer or brain stroke [3]–[8]. Moreover, the industry and academic community working on brain stroke imaging endeavor to translate this technology to a clinical setting, testing systems with different complexity on both in-lab mimicked scenarios and in clinical trials [6]–[13].

Complementing the current technologies and considering the requirements of cost and complexity, essential for future global deployment, this work presents an ad-hoc MWI prototype for the monitoring of the after-onset stroke evolution and its validation on anthropomorphic multi-tissue phantoms. This is an essential step to prove the capabilities of the system in a complex and realistic scenario, and the preamble of the pre-clinical testing. Hence, we compile here over a decade of research from feasibility studies [14], through the definition of specifications [15], and numerical studies [16], to multi-version prototyping, [17], [18], into a non-trivial and pre-clinical validation that aims to translate this technology to a clinical setting, potentially in a hospitalization bedside scenario.

In the following, Sect. II presents both the mathematical background of the imaging algorithm, the building of the imaging kernel, and the details of the low-complexity MWI prototype. Then, Sect. III covers the phantom manufacturing and the validation mimicking a hemorrhagic situation, closing up with the conclusion and perspectives in Sect. IV.

II. Microwave Imaging Prototype

A. Imaging Algorithm

The imaging algorithm is in charge of solving the inverse scattering problem that entails moving from the measured scattering parameters, ΔS, to a map of the dielectric contrast, $\Delta\chi$, of the monitored scenario, so that $\Delta S = \mathcal{L}\{\Delta\chi\}$, where $\mathcal{L}$ is the operator/kernel and frameworks of the imaging process. Specifically, the contrast is caused by the temporal variation of the dielectric properties of the brain-affected tissues, which reflects on the scattered field, and the input data are the S-parameters of an antenna array placed around the domain of interest (DoI), i.e., the head. These parameters describe the illuminating system in terms of the incoming and outgoing port waves, labeled a_p and a_q, given at the p-th and q-th antenna ports, respectively, as stated analytically by

$$\Delta S = -\frac{j\,\omega\,\varepsilon_b}{2\,a_p\,a_q}\int_{\mathrm{DoI}} \mathbf{E}_p^{ref}(\mathbf{r})\cdot\mathbf{E}_q^{ref}(\mathbf{r})\,\Delta\chi\,d\mathbf{r}, \qquad (1)$$

where j is the imaginary unit, and $\omega = 2\pi f$ is the angular frequency. The symbol "$\cdot$" denotes the dot product, and $\mathbf{E}_p^{ref}$, $\mathbf{E}_q^{ref}$ are the field distributions radiated by the p-th and q-th antennas at the time instants t_0 and t_1 in a reference scenario [19].

The kernel is then a frequency-depend integral operator that determines the quality of reached outcomes. It is usually done through full-wave simulations [16] or estimated experimentally [20]. The frequency operation is at 1 GHz, which is determined as optimal for the application and considers the trade-off between resolution and penetration [14]. Moreover, we assume "weak" and localized perturbations, taking into account that the morphological stroke phenomenon is concentrated within a region, and the differential contrast extension is determined by the pathological cadence and the examination time scheme. So, after this assumption, $\mathcal{L}$ can be linearized using a distorted Born approximation, which considers the fact that the patient's morphological specifics are unknown during an actual clinical situation. Thus, we assume an average head for building the imaging kernel.

Though $\mathcal{L}$ is linear, it is ill-conditioned, and its direct inversion is unsuitable. Accordingly, we invert and regularize it by adopting the truncated singular value decomposition (TSVD) algorithm [21] as:

$$\Delta\chi = \sum_{n=1}^{L_t}\frac{1}{\sigma_n}\,\langle\Delta S, u_n\rangle\,v_n, \qquad (2)$$

where σ_n, u_n and v_n are the n-th singular value, right and left singular vectors, respectively, obtained via the singular value decomposition (SVD) of the discretized operator $\mathcal{L}$. In (2), the truncation index L_t acts as a regularizer [21], which is set here to -30 dB considering the actual dynamic range available for the differential signal. Furthermore, ΔS is considered symmetrical as we are working with a reciprocal network, and we are dealing with linear tissues whose constitutive parameters do not depend on the field strength. As a result, S-parameters have $N(N+1)/2$ independent parameters representing the upper/lower triangular part of the matrix, where N stands for the number of antennas. However, because the non-desired variations between the antennas due to the manufacturing process are mainly evident in the reflection parameters, we exclude them from the imaging procedure. Thus, the number of independent parameters is reduced to $N(N-1)/2$, decreasing both the $\mathcal{L}$ and ΔS dimensions.

B. Low-Complexity Prototype

The MWI prototype consists of a printed helmet in clear resin (polyester casting resin), equipped with twenty-two compact and wearable monopole antennas operating at about 1 GHz [18]. The number of antennas is determined by following the design guidelines and methodology developed and tested in [15], which is an instrument to find a good trade-off between stability and accuracy based on SVD-based numerical analysis of the imaging kernel. These antennas interface with the user's head through a thin and flexible matching medium (5 mm approx.) made of a mixture of graphite and rubber with relative permittivity, $\varepsilon = 13$, and conductivity, $\sigma = 0.18$ S/m, at 1 GHz. Here, it is worth noticing that this approach is very convenient from the practical operational aspects since it avoids the use of liquids for matching and makes system maintenance and day-to-day use easier. The data acquisition system is composed of a 2-port vector network analyzer (VNA, Keysight P9375A) and an electromechanical switching matrix multiplexing the whole array, as depicted in Fig. 1. To ensure an optimal trade-off between signal-to-noise ratio and measurement time, the VNA is set with an input power of 0 dBm and the intermediate filter (IF) to 100 Hz.

Additionally, a laptop oversees the switching process, gathers the complete 22×22 scattering matrix, and executes

the imaging algorithm. The total scanning duration is approximately 6 minutes, primarily constrained by the time required for switching operations. However, updating the switches technology to solid state one will reduce its speed by at 10×, as well as its dimensions [22], [23].

III. Experimental Validation

To validate the MWI prototype in a mimicked pre-clinical scenario, we propose controlled testing using a custom-made multi-tissue anthropomorphic head, which allows checking system capabilities of the system.

The phantom consists of two material compositions, solid and liquid parts. In the case of the solid ones, these are made either from a mixture of urethane rubber and graphite powder (that is adjusted to mimic each of the head tissues by tuning their ratio) or with carbon-loaded plastic. On the other hand, the liquid components are used to represent the average dielectric properties of the brain, i.e., white and grey matter, and the stroke [24], using mixtures of water, alcohol, and salt [25]. The stroke is enclosed within a balloon that is inserted by the upper part of the head and can be externally inflated or deflated, as shown in Fig. 2. Regarding the phantom morphology, it is based on models abstracted from the Visible Human Project library, which takes computerized tomography and magnetic resonance images of human bodies' cryosections as reference [26], [27], while the dielectric reference values are taken from [28].

For the experiment, the stroke (balloon) is placed in different onset locations and filled up gradually with mimicked blood from the exterior via a thin tube attached to a syringe, mimicking an HS. This setup allows us to simulate different moments of the stroke scenario. In specific, we consider differentially the a healthy state or 0 mL, and stoke one with a 20 mL hemorrhage.

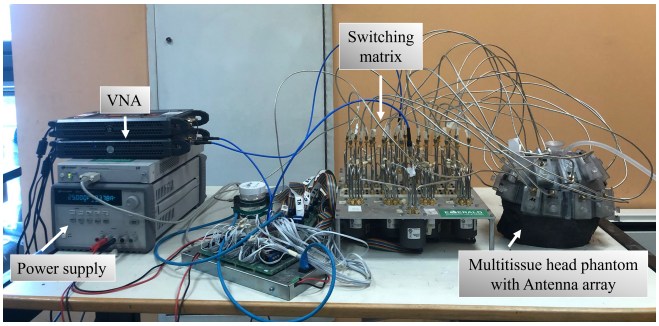

Fig. 1: Microwave imaging prototype.

Fig. 2: Multi-tissue head phantom.

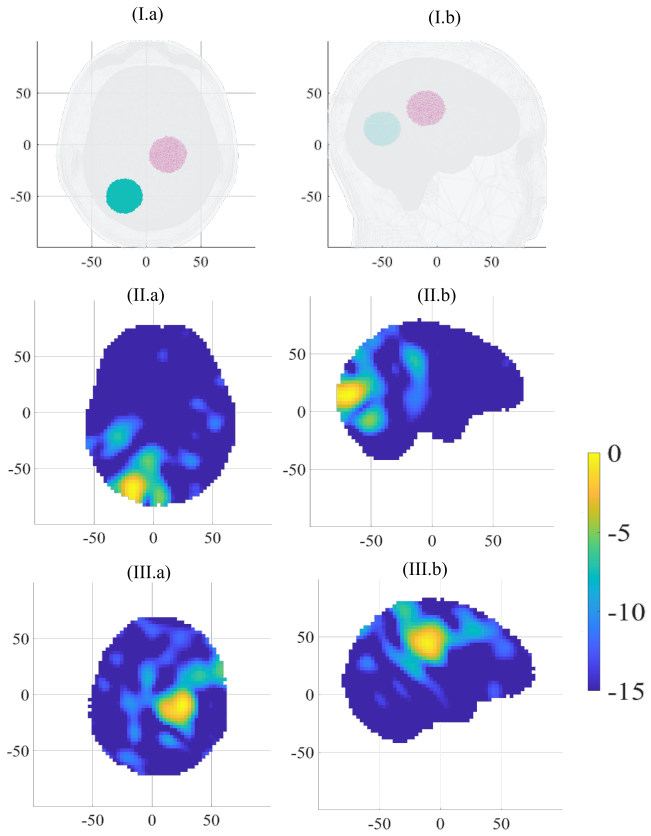

Fig. 3: Normalized reconstructed dielectric contrast sliced in the middle of the stroke region considering a transition between 0-20 mL. (I): Indication of the actual stroke position and shape. (II): *Position 1* (light blue). (III): *Position 2*(pink). (a): Transverse view. (b): Sagittal view.

In Fig. 3, we report the two cases in different stroke locations, which present the retrieved normalized dielectric contrast, sliced in the transversal (column a) and sagittal (column b) views for *Position 1* –back-left lobe– and *Position 2* –middle right lobe–. Here, it is worth recalling that the imaging operator does not consider information about the tissue morphology that is patient-dependent, i.e., it is made considering a single-tissue homogeneous head. This approach thus resembles a real clinical situation.

IV. Conclusion and Perspectives

This work presents the validation of a low-complexity MWI device, made of 22 antennas, to perform 3-D stroke imaging on a realistically mimicked in-lab scenario using a novel multi-tissue head phantom. The results demonstrate the system's reliability in terms of stroke location. For future work, we plan, first, to make a comprehensive measurement campaign, second, to extend the system's capabilities with pathology discrimination features using classification machine learning algorithms [29] and last to investigate the use of custom RF front-end systems [5].

Acknowledgment

This work was supported in part by the project PON Research and Innovation "Microwave Imaging and Detection powered by Artificial Intelligence for Medical and Industrial Applications (DM 1062/21)", funded by MUR, in part by the project "INSIGHT – An innovative microwave sensing system for the evaluation and monitoring of food quality and safety", funded by MAECI and in part by the project "THERAD - Microwave Theranostics for Alzheimer's Disease", funded by Compagnia di San Paolo. It was carried out partially within the Agritech National Research Center, funded by the European Union Next-Generation EU (Piano Nazionale di Ripresa e Resilienza (PNRR) – MISSIONE 4 COMPONENTE 2, INVESTIMENTO 1.4 – D.D. 1032 17/06/2022, CN00000022).

References

[1] "Annual report 2022," World Stroke Organization, Tech. Rep., 2022.

[2] M. O. Owolabi and et al, "Primary stroke prevention worldwide: translating evidence into action," *The Lancet Public Health*, vol. 7, no. 1, pp. e74–e85, 2022.

[3] D. O'Loughlin, M. O'Halloran, B. M. Moloney, M. Glavin, E. Jones, and M. A. Elahi, "Microwave breast imaging: Clinical advances and remaining challenges," *IEEE Transactions on Biomedical Engineering*, vol. 65, no. 11, pp. 2580–2590, 2018.

[4] L. Guo, A. S. M. Alqadami, and A. Abbosh, "Stroke diagnosis using microwave techniques: Review of systems and algorithms," *IEEE Journal of Electromagnetics, RF and Microwaves in Medicine and Biology*, pp. 1–14, 2022.

[5] M. R. Casu, M. Vacca, J. A. Tobon, A. Pulimeno, I. Sarwar, R. Solimene, and F. Vipiana, "A cots-based microwave imaging system for breast-cancer detection," *IEEE Transactions on Biomedical Circuits and Systems*, vol. 11, no. 4, pp. 804–814, 2017.

[6] "Emvision," Available at https://emvision.com.au/.

[7] "Emtensor," Available at https://www.emtensor.com/.

[8] "Ubt," Available at https://www.ubt-tech.com/.

[9] "Medfield," Available at https://www.medfielddiagnostics.com/en/.

[10] A. S. Alqadami, N. Nguyen-Trong, B. Mohammed, A. E. Stancombe, M. T. Heitzmann, and A. Abbosh, "Compact unidirectional conformal antenna based on flexible high-permittivity custom-made substrate for wearable wideband electromagnetic head imaging system," *IEEE Transactions on Antennas and Propagation*, vol. 68, no. 1, pp. 183–194, 2019.

[11] A. S. Alqadami, A. Zamani, A. Trakic, and A. Abbosh, "Flexible electromagnetic cap for three-dimensional electromagnetic head imaging," *IEEE Transactions on Biomedical Engineering*, vol. 68, no. 9, pp. 2880–2891, 2021.

[12] A. Fedeli, C. Estatico, M. Pastorino, and A. Randazzo, "Microwave detection of brain injuries by means of a hybrid imaging method," *IEEE Open Journal of Antennas and Propagation*, vol. 1, pp. 513–523, 2020.

[13] M. Salucci, A. Polo, and J. Vrba, "Multi-step learning-by-examples strategy for real-time brain stroke microwave scattering data inversion," *Electronics*, vol. 10, no. 1, p. 95, 2021.

[14] R. Scapaticci, L. D. Donato, I. Catapano, and L. Crocco, "A feasibility study on microwave imaging for brain stroke monitoring," *Progress in Electromagnetics Research*, vol. 40, pp. 305–324, 2012.

[15] R. Scapaticci, J. Tobon, G. Bellizzi, F. Vipiana, and L. Crocco, "Design and numerical characterization of a low-complexity microwave device for brain stroke monitoring," *IEEE Transactions on Antennas and Propagation*, vol. 66, no. 12, pp. 7328–7338, 2018.

[16] D. O. Rodriguez-Duarte, J. A. T. Vasquez, R. Scapaticci, L. Crocco, and F. Vipiana, "Assessing a microwave imaging system for brain stroke monitoring via high fidelity numerical modelling," *IEEE Journal of Electromagnetics, RF and Microwaves in Medicine and Biology*, vol. 5, no. 3, pp. 238–245, 2021.

[17] J. A. Tobon Vasquez, R. Scapaticci, G. Turvani, G. Bellizzi, D. O. Rodriguez-Duarte, N. Joachimowicz, B. Duchêne, E. Tedeschi, M. R. Casu, L. Crocco, and F. Vipiana, "A prototype microwave system for 3d brain stroke imaging," *Sensors*, vol. 20, no. 9, 2020.

[18] D. O. Rodriguez-Duarte, C. Origlia, J. A. T. Vasquez, R. Scapaticci, L. Crocco, and F. Vipiana, "Experimental assessment of real-time brain stroke monitoring via a microwave imaging scanner," *IEEE Open Journal of Antennas and Propagation*, vol. 3, pp. 824–835, 2022.

[19] N. K. Nikolova, *Introduction to Microwave Imaging*. Cambridge University Press, 2017.

[20] R. K. Amineh, J. J. McCombe, A. Khalatpour, and N. K. Nikolova, "Microwave holography using point-spread functions measured with calibration objects," *IEEE Transactions on Instrumentation and Measurement*, vol. 64, no. 2, pp. 403–417, 2015.

[21] M. Bertero and P. Boccacci, "Introduction to inverse problems in imaging," *CRC Press*, 1998.

[22] M. Haynes, J. Stang, and M. Moghaddam, "Real-time microwave imaging of differential temperature for thermal therapy monitoring," *IEEE Transactions on Biomedical Engineering*, vol. 61, no. 6, pp. 1787–1797, 2014.

[23] M. Ricci, B. Štitić, L. Urbinati, G. Di Guglielmo, J. A. T. Vasquez, L. P. Carloni, F. Vipiana, and M. R. Casu, "Machine-learning-based microwave sensing: A case study for the food industry," *IEEE Journal on Emerging and Selected Topics in Circuits and Systems*, vol. 11, no. 3, pp. 503–514, 2021.

[24] N. Joachimowicz, B. Duchêne, C. Conessa, and O. Meyer, "Anthropomorphic breast and head phantoms for microwave imaging," *Diagnostics*, vol. 8, no. 4, p. 85, 2018.

[25] "Ieee recommended practice for determining the peak spatial-average specific absorption rate (sar) in the human head from wireless communications devices: Measurement techniques,," p. 1–246, 2013.

[26] "Download visible human project data," Available at https://nlm.nih.gov/databases/download/vhp.html.

[27] S. N. Makarov, G. M. Noetscher, J. Yanamadala, M. W. Piazza, S. Louie, A. Prokop, A. Nazarian, and A. Nummenmaa, "Virtual human models for electromagnetic studies and their applications," *IEEE Reviews in Biomedical Engineering*, vol. 10, pp. 95–121, 2017.

[28] "An internet resource for the calculation of the dielectric properties of body tissues in the frequency range 10 Hz - 100 GHz," Available at http://niremf.ifac.cnr.it/tissprop/htmlclie/htmlclie.php.

[29] V. Mariano, J. A. Tobon Vasquez, M. R. Casu, and F. Vipiana, "Brain stroke classification via machine learning algorithms trained with a linearized scattering operator," *Diagnostics*, vol. 13, no. 1, 2023.